Published in final edited form as:
Clin Neurophysiol. 2011 June ; 122(6): 1098–1105. doi:10.1016/j.clinph.2010.10.043.

Interictal spike analysis of high density EEG in patients with partial epilepsy

Gang Wang[1,2], **Gregory Worrell**[3], **Lin Yang**[1,2], **Christopher Wilke**[1], and **Bin He**[1,2,*]

[1]Department of Biomedical Engineering, University of Minnesota, Minneapolis, Minnesota, U.S.A.

[2]Center for Neuroengineering, University of Minnesota, Minneapolis, Minnesota, U.S.A.

[3]Department of Neurology, Mayo Clinic, Rochester, Minnesota, U.S.A.

Abstract

Objective—The aim of this study is to investigate the use of interictal spikes to localize epileptogenic brain from noninvasive scalp EEG recordings in patients with medically intractable epilepsy.

Methods—Source reconstructions were performed using a high density electrode montage and a low density electrode montage by means of a distributed source modeling method. The source of interictal spike activity was localized using both realistic geometry boundary element method (BEM) head models and the 3-shell spherical head model.

Results—In the analysis of 7 patients, the high density electrode montage was found to provide results more consistent with the suspected region of epileptogenic brain identified for surgical resection using intracranial EEG recordings and structural MRI lesions, as compared to the spatial low density electrode montage used in routine clinical practice. Furthermore, the realistic geometry BEM head model provided better source localization.

Conclusions—Our results indicate the merits of using high density scalp EEG recordings and realistic geometry head modeling for source localization of interictal spikes in patients with partial epilepsy.

Significance—The present results suggest further improvement of source localization accuracy of epileptogenic brain from interictal EEG recorded using high density scalp electrode montage and realistic geometry head models.

Keywords

EEG source localization; Partial epilepsy; Localization error; Boundary element method; Interictal spike

[*]**Corresponding author:** Dr. Bin He, **Address:** Department of Biomedical Engineering, University of Minnesota, 7-105, Hasselmo Hall, 312 Church Street, Minneapolis, MN 55455, USA, **Telephone number:** +1 612 626 1115; **Fax number:** +1 612 626 6583, binhe@umn.edu (B. He).

1. Introduction

In the surgical therapy of intractable epilepsy patients, it is essential to accurately localize the epileptogenic brain generating seizures. The electrocorticogram (ECoG) recorded from subdural grid electrodes has been the gold standard for defining epileptogenic regions (Engel et al., 1981). However, the invasiveness, risk of morbidity, and high cost of this technique have stimulated the search for less invasive methods to localize the epileptogenic brain in patients with medically resistent epilepsy (Huppertz et al., 2001b). As a result, many noninvasive functional imaging methods such as functional MRI (fMRI), single photon emission computed tomography (SPECT), and positron emission tomography (PET) have been used in the presurgical assessment of epilepsy patients. Compared with these techniques, electroencephalography (EEG) remains crucial in the identification of epileptogenic regions in refractory partial epilepsy (Diekmann et al., 1998; Ding et al., 2007; Fischer et al., 2005; Worrell et al., 2000) as EEG-recorded interictal and ictal epileptiform activities are the electrophysiological signatures of epilepsy. During long-term video EEG epilepsy monitoring, interictal epileptiform spike activity is usually observed in patients with medically resistant epilepsy. Therefore, localizing the EEG generators of interictal spikes has been widely explored in an attempt to aid presurgical planning during the past several decades (Ding et al., 2006; Ebersole, 2000; Ebersole and Hawes-Ebersole, 2007; He et al., 1987; Krings et al., 1998; Lai et al., 2010; Leijten and Huiskamp, 2008; Plummer et al., 2008; Zhang et al., 2003).

In the majority of previous interictal spike studies, the routine montage of only 19–31 electrodes was used in the presurgical evaluation and was able to localize epileptogenic sources at a sublobar level (Herrendorf et al., 2000; Michel et al., 1999). Recently, a number of studies have employed high density EEG recording (more than 64 electrodes) in epilepsy patients (Brodbeck et al., 2009; Holmes 2008). However, there were few investigations that addressed the difference between using a high density montage and a low density montage for EEG source localization. Lantz et al. employed the EPIFOCUS method and SMAC model to compare the accuracy of epileptic source localization with 123, 63, and 31 electrode setups (Lantz et al., 2003a), and showed the benefit of using higher spatial sampling rate (e.g. using dense-array EEG). They did not directly evaluate the relative benefit of increasing electrode numbers while using different head models, and spike timing. In addition, because the realistic geometry head model has inherent superiority to the conventional spherical head model (Herrendorf et al., 2000; Roth et al., 1997), it is essential to study the importance of high density montage on EEG source localization using the realistic geometry head model.

In modeling the human head, the spherical head model and the boundary element method (BEM) head model have been widely applied in solving the EEG inverse problem in epilepsy patients (Ding et al., 2006; He et al., 1987; Huppertz et al., 2001b). Many investigators have suggested that the realistic geometry BEM head model improved localization accuracy as compared to the 3-shell spherical head model when using the dipole source models in patients with epilepsy (Herrendorf et al., 2000; Roth et al., 1997). Recent emphasis has been placed on developing distributed source models because they better reflect the electrophysiological reality of the EEG generators compared to dipolar sources (Plummer et al., 2008; Zumsteg et al., 2005). However, to our knowledge, no study has attempted to address the influence of different head models on epilepsy source localization using a distributed source model and high density EEG recording.

There is ongoing controversy as to which part of the interictal spike should be modeled in clinical epilepsy studies. Previous studies have shown that calculated spike sources were most reliable around the time points corresponding to the spike peaks (Mirkovic et al., 2003;

Plummer et al., 2008). However, in some cases, the rising phase of the interictal spike was considered to be most suitable for source localization (Huppertz et al., 2001a; Lantz et al., 2003b). Therefore, the selection of different time points in the source localization and their localization accuracy requires further investigation.

In the present study, we examined the ability of source imaging of interictal spikes from high density EEG recording to localize epileptogenic brain in a cohort of patients with medically intractable epilepsy. Here we identified the epileptogenic zone by using LORETA, a well adopted source localization algorithm for distributed source modeling (Pascual-Marqui et al., 1994), applied to interictal epileptiform spikes. Furthermore, we investigated the influence of electrode montage, head model, and time points of interictal spike respectively on EEG source localization in epilepsy patients. We directly compared the spatial distribution of the LORETA-calculated spike generators with the surgically resected region of brain in all patients. The goal of epilepsy surgery is to resect the epileptogenic zone, i.e. the brain region identified as the generator of the seizures. In the patients studied here the region of brain identified for surgery was selected based on chronic intracranial EEG (iEEG), MRI, and the clinical semiology of the seizures. As such, the present study was aimed at evaluating the clinical usefulness of source imaging from interictal spikes.

2. Methods

2.1. Patients and data acquisition

Seven patients with medically intractable partial epilepsy were studied using a protocol approved by the Institutional Review Boards of the University of Minnesota and Mayo Clinic. The patients reported are consecutive patients selected according to the following inclusion criteria: (1) interictal spikes recorded in high-density EEG, (2) the patients underwent resective surgery after high-density EEG monitoring, and (3) the patients underwent post-operative MRIs or there are MRI visible putative epileptogenic lesions in the pre-operative MRIs. All patients were admitted to the epilepsy monitoring unit at the Mayo Clinic (Rochester, MN, USA) and underwent presurgical evaluations that included a seizure protocol structural MRI, and both video scalp EEG and intracranial epilepsy monitoring. The location of the epileptogenic foci in each patient was identified by experienced epileptologists using high resolution anatomical MRI, ictal intracranial EEG if available, and SPECT when available. Each patient had a resection of the epileptogenic zone, and follow up at 6 months or longer after the surgical resection. Following surgical resection, six patients were seizure free and another patient experienced reduction in seizure frequency.

The scalp EEG data were recorded from 76 scalp electrodes, placed according to the modified 10–20 system, and referenced to C_z. Differential amplifiers with band-pass filters between 1Hz and 70Hz were used to minimize the effects of high frequency noise and low frequency artifacts. The sampling rate of the signals was 500Hz. The anatomical MR images (matrix size: 256×256, voxel size: 0.9375×0.9375×1.0 mm^3) were acquired on a 1.5T/3T GE Signa machine. The scalp electrode locations and the locations of three fiducial points on the head (nasion, left and right preauricular points) were digitized using a hand-held magnetic digitizer (Polhemus Inc., Colchester, VT).

2.2. Data analysis

The preoperative scalp EEG recordings were reviewed by experienced epileptologists to identify interictal spikes with similar scalp potential maps at the interictal peaks, which were segmented into artifact-free EEG epochs of 3s duration. Experienced epileptologists

performed this task via the visual inspection of the recorded data (Chatrian et al., 1974). For each patient, 8–18 interictal spikes were selected from the scalp EEG recording. The EEG data were transformed to a common average reference montage and the highest negative peak in the EEG identified. Baseline-correction was based on the scalp EEG data from 1000 to 200 ms before the negative peak of interictal discharge.

A diagram outlining the data analysis protocol is shown in Fig. 1. For the EEG data of each patient, the high density (76-electrode) montage was down-sampled to the low density (31-electrode) montage based on the clinical electrode configuration. This allowed us to subsequently analyze the interictal epileptiform spikes with high density and low density montages. For each individual spike, source distribution at the time point corresponding to the negative peak of the interictal discharge was estimated using LORETA (Ding et al., 2005; Pascual-Marqui et al., 1994; Worrell et al., 2000). The LORETA algorithm was implemented by a commercially available software package (CURRY6, Compumedics, Charlotte, NC). Solution space was defined as 3D grid inside the brain. For head modeling, the realistic geometry BEM (He et al., 1987) head model, which contains three compartments (scalp, skull, and brain), was employed (Hämäläinen and Sarvas, 1989). The surfaces (skin layer, outer skull layer, and inner skull layer) separating the three compartments were segmented from MR images using CURRY6 software (Compumedics, Charlotte, NC) for each subject. Subject-specific BEM models were then constructed from corresponding segmentation results. The conductivities of the different tissues were assumed to be 0.33 S/m for the skin, 0.0165 S/m for the skull, and 0.33 S/m for the brain (Lai et al., 2005; Zhang et al., 2006). The coregistration of EEG data and MR images, i.e. the transformation of electrode positions and MR images into the same coordinate system, was achieved by matching the digitized positions of three fiducial points (nasion, left, and right preauricular points) with the locations of these points from the MR images.

In order to study the influence of different head models on high density EEG source localization, we used the 3-shell spherical head model in the present study. The spherical model consists of 3 concentric spheres modeling the scalp, the skull, and the brain, with conductivities of 0.33 S/m, 0.0165 S/m, and 0.33 S/m, respectively. The sphere center and the radius of the outermost sphere were determined by best fitting the upper hemisphere of the outermost spherical surface onto the digitized scalp electrode locations. The relative radii of the skull and brain were 92% and 87%, respectively (Rush and Driscoll, 1969). Source reconstruction was then performed using the 3-shell spherical model and a 76-electrode montage at the negative peak time points of the interictal spikes. Subsequently, the results were compared with those we derived using the BEM model.

In epilepsy patients, the accuracy of source localization is variable across different time points of an interictal spike; however the relationship is not yet fully understood. To investigate the dynamics, we selected the spike onset and the time point of 50% from the onset-to-peak interval from each individual spike for analysis. The results were compared with those of the spike peaks. Spike onset was defined as the first significant deflection from baseline using a butterfly plot (Plummer et al., 2007). The source of interictal spike activity was subsequently localized at the spike onsets and the 50% rising time points using BEM model and high density montage.

2.3. Evaluation of EEG source localization

In this study we use the region of brain selected for surgical resection as the putative epileptogenic brain region. The brain region selected for epilepsy surgery is determined by evidence of potentially epileptogenic structural MRI lesion and intracranial EEG recording of epileptic spikes and seizures. In five patients, the resection areas were determined by co-registering the postoperative MR images with the preoperative anatomical MR images using

CURRY6 software (Compumedics, Charlotte, NC). For two patients (Patients 3 and 5) with preoperative MR images showing clear structural lesions, postoperative MR images were not available. In these two patient co-registration images of the MRI lesion and operative field was used to ensure complete resection of the MRI lesion at the time of surgery (So, 2000). The cortex around lesions is considered most likely to be the epileptogenic region (Krings et al., 1998) and MRI lesions in our subjects were consistent with the brain areas that had been subsequently removed according to the surgical report. In this case, the resection areas were obtained by delineating the structural MRI lesions. The clinical approach for epilepsy surgery is to remove the intracranial EEG determined seizure-onset zone (SOZ) and/or the entire MRI lesion (Cascino et al., 1993).

We took into account two assessment criteria to quantitatively evaluate the source localization of epileptogenic brain selected for surgery from interictal spikes. One criterion was localization error, which was determined as the shortest distance from the source location with LORETA maximum source strength to the resection areas or the MRI visible lesions. If the location with the maximum value of LORETA fell within the resection areas or the lesions, the localization error was assigned the value zero.

We used another criterion based on a receiver operating characteristic (ROC) curve to assess the overlap between the current density distribution and the resection area or lesion (Ding, 2009; Grova et al., 2006). The current density distribution obtained from the LORETA algorithm could be used to separate the estimated active region from the estimated inactive region. The resection area and the remaining whole brain could be regarded as the referenced active region and inactive region, respectively. Sensitivity and specificity were then calculated by comparing the estimated region with the referenced region. ROC curves were generated by plotting sensitivity against 1 – specificity for different thresholds. The area under the ROC curve (AUC) can be used to evaluate the concordance between the current density distribution and the resected region. The larger the AUC value the more consistent the overlap between the estimated source distribution and the epileptogenic brain selected for surgery. To obtain a less biased estimation of the AUC, one should theoretically provide the same number of referenced active and inactive sources to estimate ROC parameters. We used a method reported in Grova et al., 2006 to solve this problem. The AUC was measured by randomly choosing a subset of referenced inactive sources with the same number as referenced active sources. This random selection was repeated 50 times and the AUC index used in the present study is the mean AUC over these 50 trials.

In order to compare source localization differences resulting from electrode montage, head model, and time point of interictal spikes, one-way analysis of variance (ANOVA) (Wang et al., 2006a; Wang et al., 2006b) was used. The ANOVA procedure can help determine whether observed differences in source localization accuracy are attributed to the advantages of each method. It is well known that the EEG signals are subject-dependent, thus the ANOVA is performed according to the response of each subject. In this paper significance level was set at $p < 0.05$.

3. Results

The clinical information of the 7 patients is summarized in Table 1. The locations of LORETA maximum source strength from all interictal spikes in Patient 1 are shown in Fig. 2. Different color dots denote the source locations with LORETA maximum source strength from different interictal spikes. The yellow curves refer to the boundaries of surgically resected brain area. From the source localization results using the BEM head model and 76-electrode montage (Fig. 2A), it can be observed that most of color dots are located inside the resected regions and the other dots although localized outside of the resected region are also

very close to the boundaries. Comparing source imaging results showed in Fig. 2, using the BEM head model and 76-electrode montage (Fig. 2A) performed better source detection than using the 31-electrode montage (Fig. 2B) or using the spherical head model (Fig. 2C). Source localization results in the remaining six patients are illustrated in Fig. 3. For each patient, the results showed the same trend as Fig. 2.

3.1. Comparison of high density montage with low density montage

Fig. 4 shows the numerical differences between the source localization accuracy of the high density montage and the low density montage in all seven patients. The mean and standard deviation values of localization errors and AUC indexes for all interictal spikes of each individual patient are represented in Fig. 4A and B respectively, where the realistic geometry BEM head model was used for each patient. For all seven patients, the mean localization errors ranged between 3.69 and 7.76 mm with the 76-electrode montage and between 8.56 and 15.72 mm with the 31-electrode montage. The mean AUC indexes ranged between 0.9344 and 0.9828 with the 76-electrode montage and between 0.7899 and 0.9546 with the 31-electrode montage.

When we compared the source localization performance of the high density montage with the low density montage, a one-way ANOVA was used. The high density montage resulted in significantly less localization errors than the low density montage in all patients. Additionally, the AUC indexes of the high density montage were significantly larger than those with the low density montage in all patients.

3.2. Comparison between BEM head model and spherical head model

The localization differences between the BEM head model and the 3-shell spherical head model are illustrated in Fig. 5, when 76-electrode montage was used. For the BEM head model, the mean localization errors were between 3.69 and 7.76 mm, and the mean AUC indexes were between 0.9344 and 0.9828. In case of the spherical head model, the mean localization errors were between 7.59 and 18.59 mm, and the mean AUC indexes using spherical model were between 0.84 and 0.91. In terms of source localization accuracy, the superiority of the realistic geometry head model was statistically significant when compared with the spherical head model in all patients expect two (Patient 3 for localization error, Patient 4 for AUC index).

3.3. Comparison among the spike onset, the 50% rising time point, and the spike peak

The 76 electrode montage and the realistic geometry BEM head model were used in this comparison study. In all seven patients, the localization results at the spike onsets were far from the patient epileptogenic regions according to our analysis. Therefore, we just show the differences of source localization between the spike peaks and the 50% rising time points in Fig. 6. The mean localization errors of the 50% rising time points were between 13.51 and 19.93 mm. The mean AUC indexes of the 50% rising time points were between 0.71 and 0.822. The localization errors at the spike peaks were significantly less than those at the 50% rising time points in all patients. In terms of AUC index, the localization results using spike peaks were significantly superior when compared to the 50% rising time points in six of the patients, while the one remaining case showed no significant difference between the two time points.

4. Discussion

In this study, we have examined the effects of number of scalp electrodes, head models, and selection of time points on the identification of the epileptogenic region, with the use of LORETA algorithm. Specifically, we studied 7 patients who underwent surgical evaluation

for the treatment of medically intractable partial epilepsy. In 6 of the 7 patients, the resected areas were located within the temporal lobe. For one patient, the resected area was within the frontal lobe. Long-term EEG video monitoring based on configurations with 19–30 scalp electrodes is the routine presurgical workup in patients with epilepsy. With an increased number of electrodes, EEG data can provide improved spatial resolution, and information of the epileptogenic zone in human brain (Holmes, 2008). Our results verified the possibility of enhancing source localization accuracy and consistency with the region of epileptogenic brain selected for surgical resection when using a high density electrode montage in epilepsy patients.

Several studies have previously shown that dipole source models have been successfully used to detect the epileptogenic foci of interictal epileptiform activity (Ebersole and Hawes-Ebersole, 2007; Gavaret et al., 2009; Huppertz et al., 2001b). Recently, distributed source models have gained popularity in solving the EEG inverse problem since they regard cerebral sources as physiologically more plausible extended active brain regions. Consistent with this practice we used a validated distributed modeling algorithm (LORETA) to perform source reconstruction in this study. It has been demonstrated that the localization accuracy of the BEM head model is superior to the 3-shell spherical head model when using dipolar source localization as the BEM model can more precisely model the shape of 3 piece-wise homogeneous head compartments in the individual brain (Roth et al., 1997; Silva et al., 1999). Our results extend this conclusion to the distributed models.

When selecting the analyzed time point of interictal spikes in epilepsy source reconstruction, we consider the effect of two factors on localization accuracy: the signal to noise ratio (SNR) and the epileptiform propagation. Our results indicate that the spike peak appears to be more appropriate for source localization since SNR of the EEG signal is highest at the time points of spike peaks. On the other hand, interictal epileptiform activity could propagate within several milliseconds to relatively remote cortex during the onset-to-peak interval of interictal spike (Alarcon et al., 1994). The onset or the rising phase of the interictal spike would give more accurate source localization results. There is a tradeoff when selecting among spike peak, spike onset and spike rising phrase. Our study has shown that the spike peak gave the best source localization results when compared with the spike onset and the 50% rising time points. This may be explained by the fact that the propagation of interictal epileptiform activity is around the resected areas or the MRI visible lesions for the patients in our study. The high SNR of the spike peak results in better localization accuracy than the spike onset and the 50% rising time points. The localization accuracy is mainly influenced by SNR rather than propagation in this study. However, it is possible that in some patients the interictal epileptiform activity would propagate to other regions of the brain during the onset-to-peak interval. In this case, the peak instant may not give the best estimation of the spike source, and we should select the time point for source localization carefully.

In addition to electrode montage, head model, and time points of interictal spike, recent studies have suggested that skull holes may also have impact on EEG source localization (Heasman et al., 2002; Sparkes et al., 2009). Sparkes et al. (2009) reported that skull holes play a role in the transmission to the scalp of epileptiform discharges and they suggested that facial and anterior temporal electrodes should be used to acquire EEG signals for localizing the epileptogenic sources in temporal lobe epilepsy. The effect of skull holes to EEG source localization remains to be further studied.

Localization error is a widely used criterion to evaluate the performance of source localization in epilepsy patients. However, when the distributed modeling method is used to solve the EEG inverse problem, one should consider not only the localization error between

the epileptogenic brain and the maximum source strength location, but also the overlap between the estimated current density distribution and the epileptogenic area. The AUC index used in the present study is one criterion that can assess the accuracy of estimated source distribution. From the results, it was observed that the localization errors from the BEM head model were not significantly less than those from the spherical head model in Patient 3 (Fig. 5A). Nevertheless, the AUC indexes from the BEM head model were significantly larger than those from the spherical head model in this patient (Fig. 5B). The opposite situation was also found in Patient 4 (Fig. 5). The AUC index is a criterion different from the localization error and gives information that the localization error does not include. Fig. 4 shows that the AUC of Patient 2 is larger than that of Patient 3 (Fig. 4B) while the localization error of Patient 2 is smaller than that of Patient 3 (Fig. 4A). This discrepancy suggested that the estimated source distribution in Patient 2 overlaps better with the resected region than in Patient 3, while the maximal estimated source point in Patient 3 localized closer to the resected region than in Patient 2. As such, when using distributed source model for source imaging, it is desirable to employ the AUC index.

In summary, we have found that the use of the LORETA algorithm on interictal spike activity obtained from high-density EEG recordings was able to accurately localize epileptogenic sources as assessed by the brain regions ultimately selected for surgical resection. In the seven patients studied, the accuracy of source localization from a 76-electrode montage was substantially better than that recorded in a 31-electrode montage, as judged from surgical resection results. Additionally, the realistic geometry BEM head model was found to provide results more consistent with the resected areas than the 3-shell spherical head model. Source localization was most accurate at the spike peak as compared to spike onset and 50% rising time points. These findings indicate the merits of high density EEG recordings, realistic geometry head modeling and the use of spike peak for source localization of interictal spikes in epilepsy patients. Currently, low-density EEG, high resolution MRI, intracranial EEG have been used in presurgical evaluation in order to obtain optimal surgical outcome. Our results suggest that using high density EEG recording and the source imaging technique would promise to further our efforts to identify epileptogenic brain in the treatment of medically intractable epilepsy.

Acknowledgments

The authors would like to thank Cindy Nelson for technical assistance in data collection, and Dr. Benjamin Brinkmann for assistance in data mining. This work was supported in part by NIH RO1EB007920, NIH RO1EB006433, and a grant from the Minnesota Partnership for Biotechnology and Medical Genomics.

References

Alarcon G, Guy CN, Binnie CD, Walker SR, Elwes RDC, Polkey CE. Intracerebral propagation of interictal activity in partial epilepsy: implications for source localisation. J Neurol Neurosur PS. 1994; 57:435–449.

Brodbeck V, Lascano A, Spinelli L, Seeck M, Michel C. Accuracy of EEG source imaging of epileptic spikes in patients with large brain lesions. Clin Neurophysiol. 2009; 120:679–685. [PubMed: 19264547]

Cascino, GD.; Boon, P.; Fish, DR. Surgically remedial lesional syndromes. In: Engel, JJ., editor. Surgical treatment of the epilepsies. New York: Raven Press; 1993.

Chatrian G, Bergamini L, Dondey M, Klass D, Lennox-Buchtal MIP. A glossary of terms most commonly used by clinical electroencephalographers. Electroencephalogr Clin Neurophysiol. 1974; 37:538–548. [PubMed: 4138729]

Diekmann V, Becker W, Jürgens R, Grözinger B, Kleiser B, Richter H, Wollinsky K. Localisation of epileptic foci with electric, magnetic and combined electromagnetic models. Electroencephalogr Clin Neurophysiol. 1998; 106:297–313. [PubMed: 9741758]

Ding L. Reconstructing cortical current density by exploring sparseness in the transform domain. Phys Med Biol. 2009; 54:2683–2697. [PubMed: 19351982]

Ding L, Lai Y, He B. Low resolution brain electromagnetic tomography in a realistic geometry head model: a simulation study. Phys Med Biol. 2005; 50:45–56. [PubMed: 15715421]

Ding L, Worrell G, Lagerlund T, He B. 3D source localization of interictal spikes in epilepsy patients with MRI lesions. Phys Med Biol. 2006; 51:4047–4062. [PubMed: 16885623]

Ding L, Worrell G, Lagerlund T, He B. Ictal source analysis: localization and imaging of causal interactions in humans. Neuroimage. 2007; 34:575–586. [PubMed: 17112748]

Ebersole J. Noninvasive localization of epileptogenic foci by EEG source modeling. Epilepsia. 2000; 41 Suppl 3:S24–S33. [PubMed: 11001333]

Ebersole J, Hawes-Ebersole S. Clinical application of dipole models in the localization of epileptiform activity. J Clin Neurophysiol. 2007; 24:120–129. [PubMed: 17414967]

Engel JJ, Rausch R, Lieb J, Kuhl D, Crandall P. Correlation of criteria used for localizing epileptic foci in patients considered for surgical therapy of epilepsy. Ann Neurol. 1981; 9:215–224. [PubMed: 7013652]

Fischer M, Scheler G, Stefan H. Utilization of magnetoencephalography results to obtain favourable outcomes in epilepsy surgery. Brain. 2005; 128:153–157. [PubMed: 15563514]

Gavaret M, Trébuchon A, Bartolomei F, Marquis P, McGonigal A, Wendling F, Regis J, Badier J, Chauvel P. Source localization of scalp-EEG interictal spikes in posterior cortex epilepsies investigated by HR-EEG and SEEG. Epilepsia. 2009; 50:276–289. [PubMed: 18717708]

Grova C, Daunizeau J, Lina J, Bénar C, Benali H, Gotman J. Evaluation of EEG localization methods using realistic simulations of interictal spikes. Neuroimage. 2006; 29:734–753. [PubMed: 16271483]

He B, Musha T, Okamoto Y, Homma S, Nakajima Y, Sato T. Electric dipole tracing in the brain by means of the boundary element method and its accuracy. IEEE Trans Biomed Eng. 1987; 34:406–414. [PubMed: 3610187]

Heasman BC, Valentin A, Alarcon G, Garcia Seoane JJ, Binnie CD, Guy CN. A hole in the skull distorts substantially the distribution of extracranial electric fields in an in vitro model. J Clin Neurophys. 2002; 19:163–171.

Herrendorf G, Steinhoff B, Kolle R, Baudewig J, Waberski T, Buchner H, Paulus W. Dipole-source analysis in a realistic head model in patients with focal epilepsy. Epilepsia. 2000; 41:71–80. [PubMed: 10643927]

Holmes M. Dense array EEG: methodology and new hypothesis on epilepsy syndromes. Epilepsia. 2008; 49 Suppl 3:3–14. [PubMed: 18304251]

Huppertz H, Hoegg S, Sick C, Lücking C, Zentner J, Schulze-Bonhage A, Kristeva-Feige R. Cortical current density reconstruction of interictal epileptiform activity in temporal lobe epilepsy. Clin Neurophysiol. 2001a; 112:1761–1772. [PubMed: 11514259]

Huppertz H, Hof E, Klisch J, Wagner M, Lücking C, Kristeva-Feige R. Localization of interictal delta and epileptiform EEG activity associated with focal epileptogenic brain lesions. Neuroimage. 2001b; 13:15–28. [PubMed: 11133305]

Hämäläinen M, Sarvas J. Realistic conductivity geometry model of the human head for interpretation of neuromagnetic data. IEEE Trans Biomed Eng. 1989; 36:165–171. [PubMed: 2917762]

Krings T, Chiappa K, Cuffin B, Buchbinder B, Cosgrove G. Accuracy of electroencephalographic dipole localization of epileptiform activities associated with focal brain lesions. Ann Neurol. 1998; 44:76–86. [PubMed: 9667595]

Lai Y, van Drongelen W, Ding L, Hecox K, Towle V, Frim D, He B. Estimation of in vivo human brain-to-skull conductivity ratio from simultaneous extra- and intra-cranial electrical potential recordings. Clin Neurophysiol. 2005; 116:456–465. [PubMed: 15661122]

Lai Y, Zhang X, van Drongelen W, Korhman M, Hecox K, Ni Y, He B. Noninvasive Cortical Imaging of Epileptiform Activities from Interictal Spikes in Pediatric Patients. Neuroimage. 2010 in press.

Lantz G, Grave de Peralta R, Spinelli L, Seeck M, Michel C. Epileptic source localization with high density EEG: how many electrodes are needed? Clin Neurophysiol. 2003a; 114:63–69. [PubMed: 12495765]

Lantz G, Spinelli L, Seeck M, de Peralta Menendez R, Sottas C, Michel C. Propagation of interictal epileptiform activity can lead to erroneous source localizations: a 128-channel EEG mapping study. J Clin Neurophysiol. 2003b; 20:311–319. [PubMed: 14701992]

Leijten F, Huiskamp G. Interictal electromagnetic source imaging in focal epilepsy: practices, results and recommendations. Curr Opin Neurol. 2008; 21:437–445. [PubMed: 18607204]

Michel C, Grave de Peralta R, Lantz G, Gonzalez Andino S, Spinelli L, Blanke O, Landis T, Seeck M. Spatiotemporal EEG analysis and distributed source estimation in presurgical epilepsy evaluation. J Clin Neurophysiol. 1999; 16:239–266. [PubMed: 10426407]

Mirkovic N, Adjouadi M, Yaylali I, Jayakar P. 3-d source localization of epileptic foci integrating EEG and MRI data. Brain Topogr. 2003; 16:111–119. [PubMed: 14977204]

Pascual-Marqui R, Michel C, Lehmann D. Low resolution electromagnetic tomography: a new method for localizing electrical activity in the brain. Int J Psychophysiol. 1994; 18:49–65. [PubMed: 7876038]

Plummer C, Harvey A, Cook M. EEG source localization in focal epilepsy: where are we now? Epilepsia. 2008; 49:201–218. [PubMed: 17941844]

Plummer C, Litewka L, Farish S, Harvey A, Cook M. Clinical utility of current-generation dipole modelling of scalp EEG. Clin Neurophysiol. 2007; 118:2344–2361. [PubMed: 17889598]

Roth B, Ko D, von Albertini-Carletti I, Scaffidi D, Sato S. Dipole localization in patients with epilepsy using the realistically shaped head model. Electroencephalogr Clin Neurophysiol. 1997; 102:159–166. [PubMed: 9129570]

Rush S, Driscoll D. EEG electrode sensitivity--an application of reciprocity. IEEE Trans Biomed Eng. 1969; 16:15–22. [PubMed: 5775600]

Silva C, Almeida R, Oostendorp T, Ducla-Soares E, Foreid J, Pimentel T. Interictal spike localization using a standard realistic head model: simulations and analysis of clinical data. Clin Neurophysiol. 1999; 110:846–855. [PubMed: 10400198]

So EL. Integration of EEG, MRI, and SPECT in localizing the seizure focus for epilepsy surgery. Epilepsia. 2000; 41 Suppl 3:S48–S54. [PubMed: 11001336]

Sparkes M, Valentín A, Alarcón G. Mechanisms involved in the conduction of anterior temporal epileptiform discharges to the scalp. Clin Neurophysiol. 2009; 120:2063–2070. [PubMed: 19850514]

Wang G, Wang Z, Chen W, Zhuang J. Classification of surface EMG signals using optimal wavelet packet method based on Davies-Bouldin criterion. Med Biol Eng Comput. 2006a; 44:865–872. [PubMed: 16951931]

Wang G, Yan Z, Hu X, Xie H, Wang Z. Classification of surface EMG signals using harmonic wavelet packet transform. Physiol Meas. 2006b; 27:1255–1267. [PubMed: 17135698]

Worrell G, Lagerlund T, Sharbrough F, Brinkmann B, Busacker N, Cicora K, O'Brien T. Localization of the epileptic focus by low-resolution electromagnetic tomography in patients with a lesion demonstrated by MRI. Brain Topogr. 2000; 12:273–282. [PubMed: 10912735]

Zhang X, van Drongelen W, Hecox K, Towle V, Frim D, McGee A, He B. High-resolution EEG: cortical potential imaging of interictal spikes. Clin Neurophysiol. 2003; 114:1963–1973. [PubMed: 14499758]

Zhang Y, van Drongelen W, He B. Estimation of in vivo brain-to-skull conductivity ratio in humans. Appl Phys Lett. 2006; 89:223903–2239033. [PubMed: 17492058]

Zumsteg D, Friedman A, Wennberg R, Wieser H. Source localization of mesial temporal interictal epileptiform discharges: correlation with intracranial foramen ovale electrode recordings. Clin Neurophysiol. 2005; 116:2810–2818. [PubMed: 16253551]

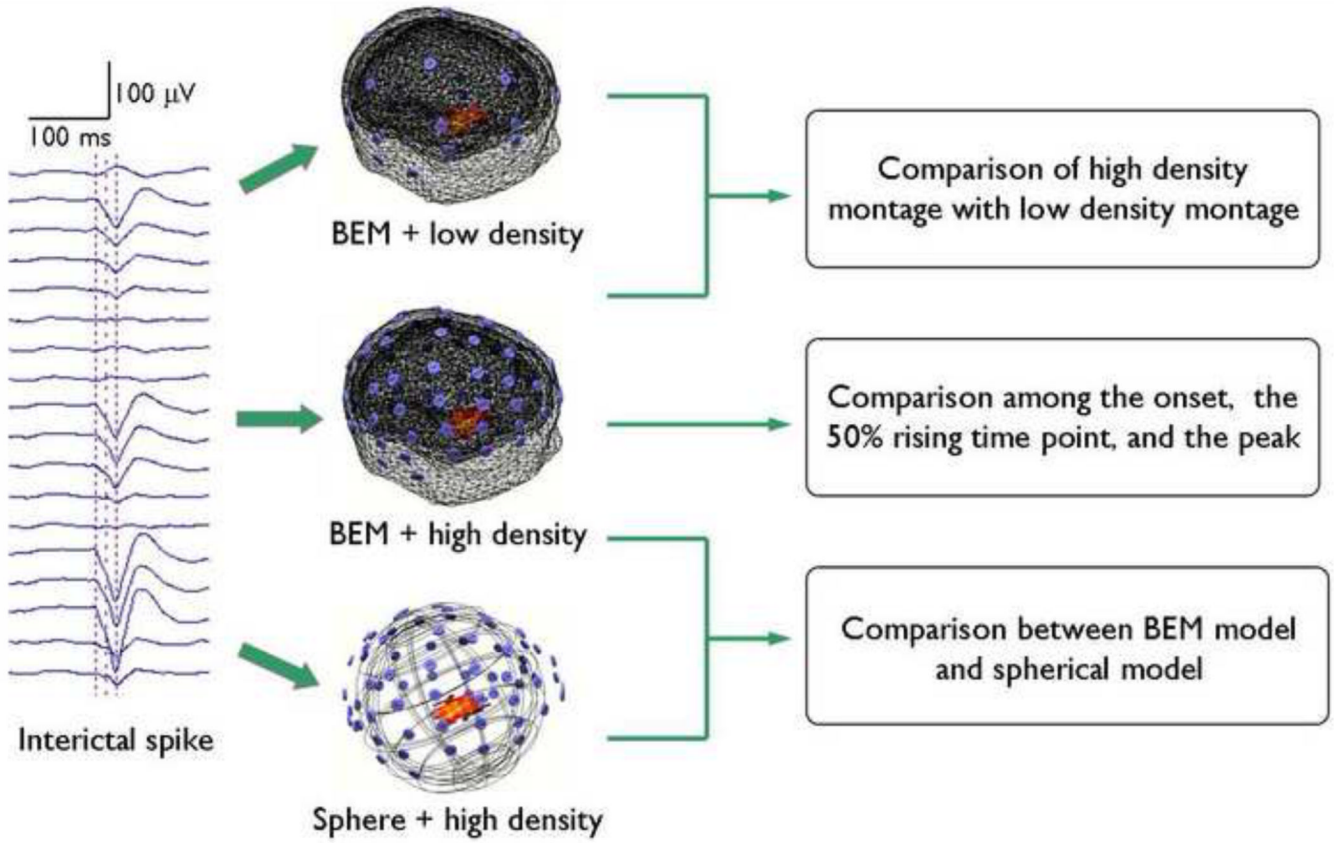

Fig.1.
The protocol of the present data analysis.

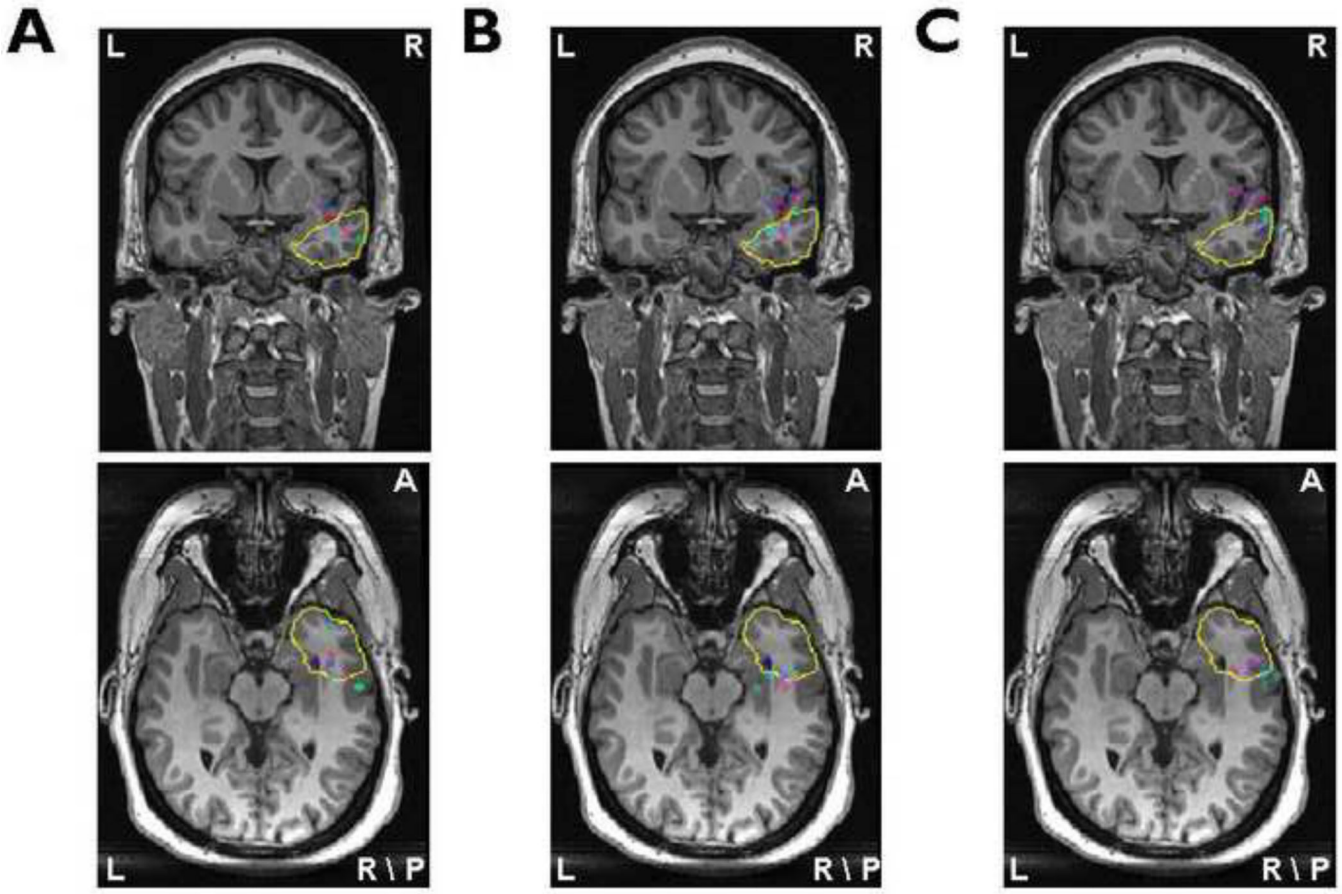

Fig.2.

The source locations of all interictal spikes in Patient 1 obtained from the BEM model / 76-electrode montage (A), the BEM model / 31-electrode montage (B) and the spherical model / 76-electrode montage (C). All source localization results are projected onto corresponding preoperative MR images. The yellow lines illustrate the boundaries of resection areas or lesions. Different color dots represent the locations of LORETA maximum source strength from all interictal spikes of Patient 1.

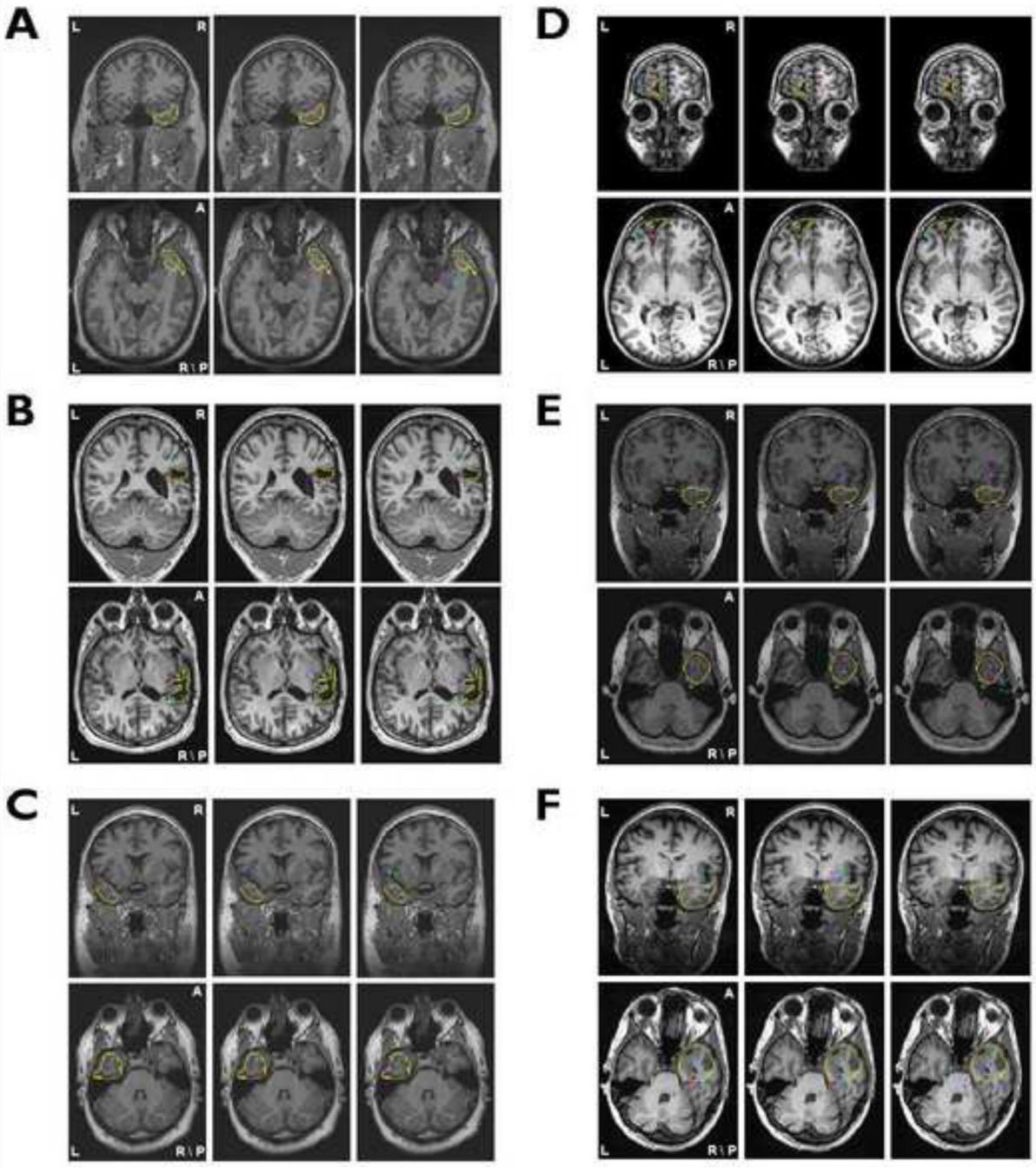

Fig.3.

The source localization results projected on corresponding preoperative MR images for Patient 2 (A) through Patient 7(F). The layout of the results for each patient is the same as shown in Fig. 2.

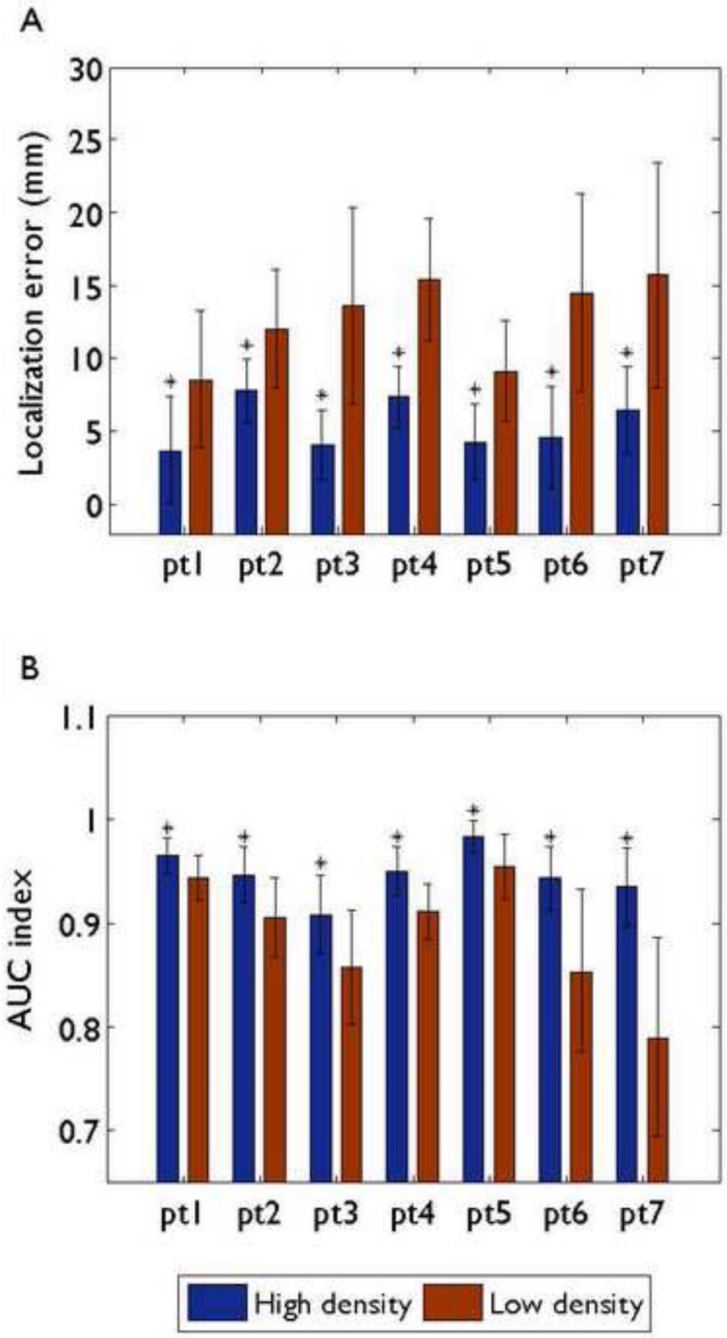

Fig.4.

Comparison of localization errors (A) and AUC indexes (B) between the 76-electrode montage and the 31-electrode montage for each patient using the realistic geometry BEM head model. Mean values corresponding to different montages are represented by different color bars. Black bars: standard deviations. An asterisk indicates that the results of the 76-electrode montage are significantly better than those with the 31-electrode montage.

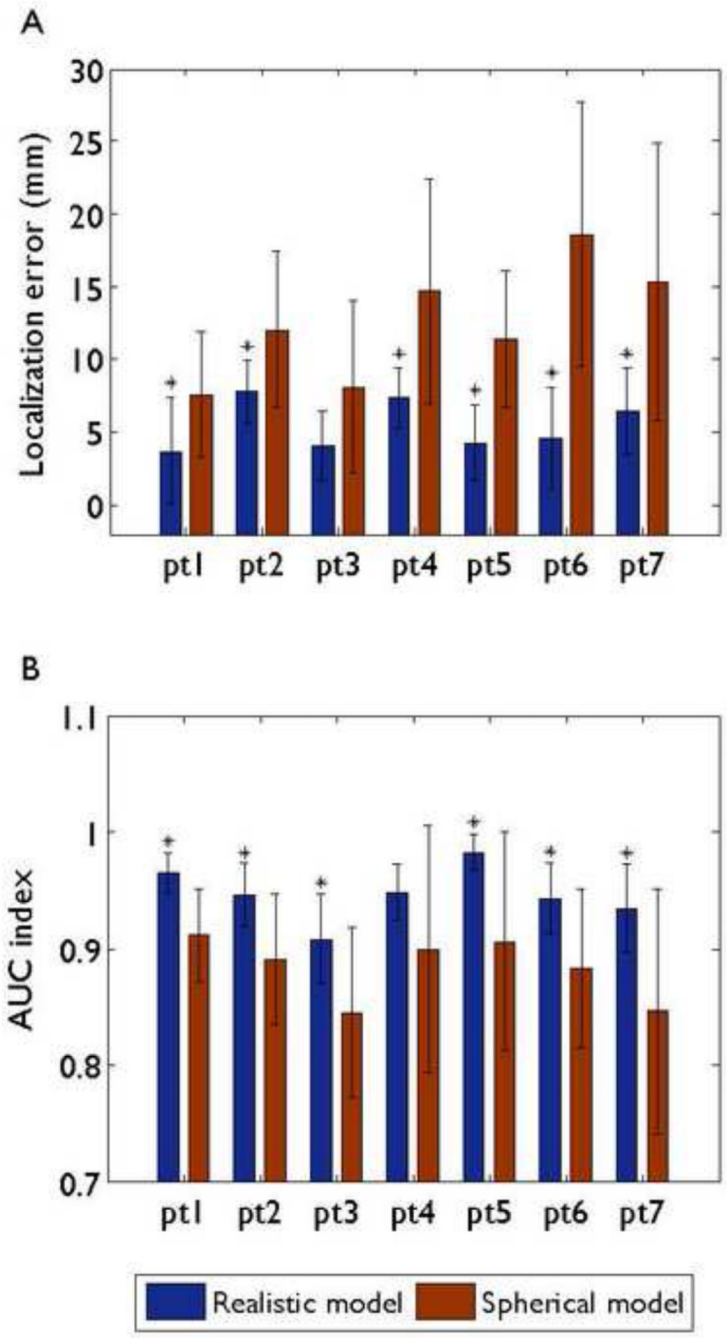

Fig.5.

Comparison of localization errors (A) and AUC indexes (B) between the BEM head model and the 3-shell spherical head model for each patient when 76-electrode montage was used. Mean values corresponding to different models are represented by different color bars. Black bars: standard deviations. An asterisk indicates that the results of the BEM head model are significantly better than those with the 3-shell spherical head model.

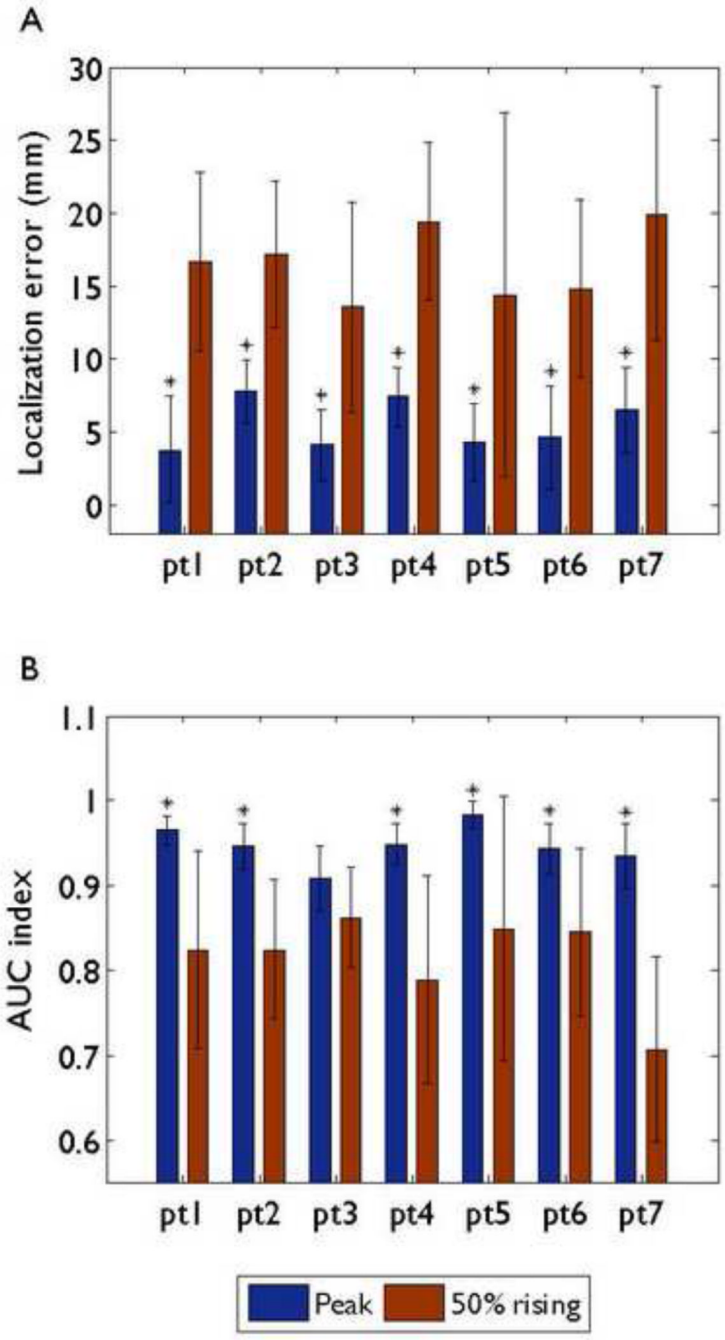

Fig.6.

Comparison of localization errors (A) and AUC indexes (B) between the spike peak and the 50% rising time point for each patient using 76 electrode montage and the BEM head model. Mean values corresponding to different time points are represented by different color bars. Black bars: standard deviations. An asterisk indicates that the results at the spike peaks are significantly better than those at the 50% rising time points.

Table 1

Clinical information for all patients

Patient	Gender	Age of onset	Age at surgery	Surgery	Ictal EEG localization	Imaging findings (Seizure protocol MRI, PET and SPECT)	Pathology	Outcome	Duration of follow-up
1	Female	22	33	Right temporal lobectomy	Right temporal	Bilateral increased T_2 signal in HC without evidence of atrophy.	Hippocampus: Mesial temporal sclerosis.	ILAE-1	14 months
2	Male	21	26	Right temporal lobectomy	Right temporal	Scattered foci of T2 hyperintensity in the right centrum semiovale and central Pons. Ill-defined area along the superior margin of the right lateral ventricle frontal horn FDG PET: Decreased metabolism right temporal lobe	Right Temporal lobe: Severe subpial and subcortical gliosis Hippocampus: severe gliosis.	ILAE-1	23 months
3	Male	21	25	Right temporal cortical resection	right centroparietal	Post-surgical changes of right temporoparietal region. Prior craniotomy, for a right parietal AVM, encephalomalacia in the subjacent brain, and ex vacuo dilatation of the right lateral ventricle.	Right frontal and temporal lobe: chronic subpial gliosis; Superficial cortical microinfarctions; occasional vessels containing embolic material White matter gliosis	ILAE-5	11 months
4	Male	11 Months	32	Left temporal lobectomy	Left temporal	MRI: Left HC Atrophy and T2 signal	Left Hippocampus: mesial temporal sclerosis.	ILAE-1	22 months
5	Female	17	22	Left frontopolar resection	Left frontal polar	MRI: Left frontal polar encephalomalcia	Sub cortical and subpial gliosis	ILAE-1	6 months
6	Female	6	21	Right temporal lobectomy	Right temporal	Normal	Moderate subpial and subcortical gliosis; Right Hippocampus: mesial temporal sclerosis.	ILAE-1	13 months
7	Female	11 Months	46	Right temporal lobectomy	Right temporal	Negative except for mild generalized cerebellar atrophy.	Right Temproal Lobe and HC: Severe diffuse cortical, mesial temporal and HC gliosis	ILAE-2	15 months

ILAE: International League Against Epilepsy

Clin Neurophysiol. Author manuscript; available in PMC 2012 June 1.